Density evolution of the picosecond time-domain CARS responses from carbon dioxide gas

ARTICLE *in* JOURNAL OF RAMAN SPECTROSCOPY · DECEMBER 2003

Impact Factor: 2.67 · DOI: 10.1002/jrs.1097

5 AUTHORS, INCLUDING:

V. B. Morozov
Lomonosov Moscow State University
57 PUBLICATIONS **227** CITATIONS
SEE PROFILE

V. G. Tunkin
Lomonosov Moscow State University
98 PUBLICATIONS **506** CITATIONS
SEE PROFILE

Alexander P Kouzov
Saint Petersburg State University
75 PUBLICATIONS **237** CITATIONS
SEE PROFILE

JOURNAL OF RAMAN SPECTROSCOPY
J. Raman Spectrosc. 2003; **34**: 983–988
Published online in Wiley InterScience (www.interscience.wiley.com). DOI: 10.1002/jrs.1097

JRS

Density evolution of the picosecond time-domain CARS responses from carbon dioxide gas

V. Morozov,[1] S. Mochalov,[1] A. Olenin,[1] V. Tunkin[1] and A. Kouzov[2]*

[1] Department of Physics, Moscow State University, Moscow 119992, Russia
[2] Institute of Physics, St. Petersburg State University, Peterhof, St. Petersburg 198504, Russia

Received 31 May 2003; Accepted 20 August 2003

Results of a joint experimental and theoretical study of CARS transients produced by picosecond two-color pumping of the CO_2 Q-branch at 1285 cm^{-1} are reported. The coherence decay patterns recorded in a wide dynamic range (3–8 decades) and in a broad gas density interval (ρ = 0.02–20 amagat) made it possible to track different channels of collision-induced relaxation. The undertaken signal simulations account for the finite pump–probe pulse durations and also for the collision-perturbed Doppler effect, vibrational dephasing and collisional mixing of rotational states. The last effect was tackled by applying the quantum fast-collision model of rotational relaxation. Our recent data on the other Fermi-dyad component at 1388 cm^{-1} were also simulated in the same way to derive a set of optimized relaxation rate parameters. New features revealed at low densities are ascribed to interference between the velocity and rotational relaxation channels. Copyright © 2003 John Wiley & Sons, Ltd.

KEYWORDS: time-domain CARS spectroscopy; molecular relaxation; molecular collisions; carbon dioxide

INTRODUCTION

Despite the recent impressive encroach of CARS on the femtosecond province,[1] the picosecond (PS) time domain remains insufficiently explored by this promising technique. However, it is the ps scale in which the Raman coherence responses from many practically important molecular gases evolve and decay. These signals produce a detailed fingerprint of how the rotovibrational and translational degrees of freedom develop in time[2] and become perturbed and coupled because of collisions.

Since CARS is a non-linear optical method, the data obtained by the frequency- and time-resolved CARS techniques cannot be directly interconverted and mostly they complement each other. Although intrinsically such data are influenced by the same processes, the time-domain studies offer additional benefits to investigators. First, their sensitivity is substantially higher than in the frequency-domain CARS case, which allows one to track the coherence decays in a much larger dynamic range (almost nine decades). Second, the parasitic responses due to electronic non-resonant non-linear susceptibility dissapear almost instantly and, provided the pump and probe pulses are short enough, can be effectively separated from the useful signals. Finally, variations in gas density permit one to track different relaxation effects (velocity, rotation, vibration) more clearly than one can do using the frequency-resolved CARS spectra.

Because of the technological and environmental importance of carbon dioxide, its spectra have been studied by numerous continuous-wave techniques including CARS. Owing to them, the CO_2 spectroscopic constants are accurately known.[3] Therefore, interpretation of the ideal-gas responses meets no problem and allows us to concentrate on the collisional effects. It is also important that CO_2 has narrow Q-branches easily accessible by ps CARS techniques.

EXPERIMENTAL

The scheme and detailed description of the CARS spectrometer have been given previously.[4,5] Single second-harmonic picosecond pulses of an Nd : YAG laser (0.532 nm, 25 ps and 2 mJ) and a dye laser (0.57 nm, 30 ps and 1 mJ) were used to excite the studied transitions, which were probed by the third harmonic pulses (0.355 nm and 0.2 mJ). The pump and probe beams were focused collinearly into a CO_2-containing cell using a lens with a focal length of 30 cm. The polarizations of the exciting beams were parallel to each other, with the polarization of the probe beam perpendicular to them. The anti-Stokes radiation was filtered off by a double grating monochromator and recorded with a photomultiplier.

*Correspondence to: A. Kouzov, Institute of Physics, St. Petersburg State University, Peterhof, St. Petersburg 198504, Russia.
E-mail: alex@apk.usr.pu.ru
Contract/grant sponsor: Russian Foundation for Basic Research;
Contract/grant numbers: 01-02-16044; 01-03-32744.

JRS

New room-temperature ($T = 298$ K) experimental data on the isotropic ps CARS responses from the CO_2 1285 cm^{-1} band (the 'red' Fermi-dyad component) in a wide density range ($\rho \approx 2 \times 10^{-2}$–20 amagat) are reported. Along with the simulated signals they are displayed in Figs 1 and 2. Previously, similar ps studies were performed at Moscow State University at $\rho \approx 10^{-3}$–20 amagat on the 1388 cm^{-1} band (the 'blue' Fermi-dyad component).[4] These data are also included in the present analysis.

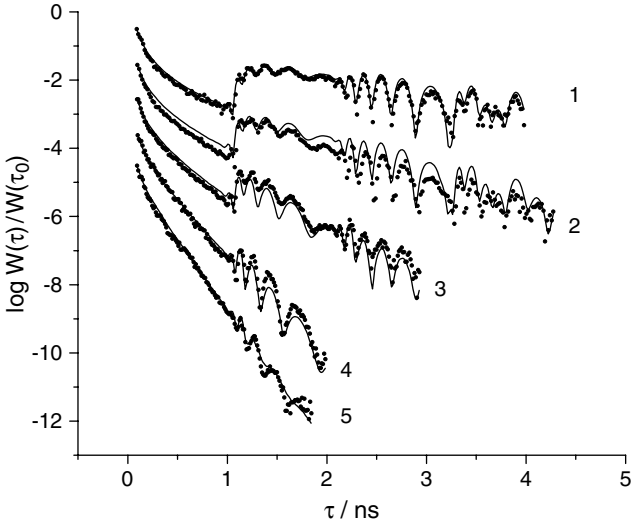

Figure 1. Raman coherence signals obtained on 1285 cm^{-1} band excitation ($T = 298$ K). Displayed are experimental (dots) and simulated (solid lines) values; gas densities: (1) 0.024; (2) 0.047; (3) 0.094; (4) 0.189; (5) 0.283 amagat. For clarity, curves 2–5 are sequentially shifted downwards by 1.

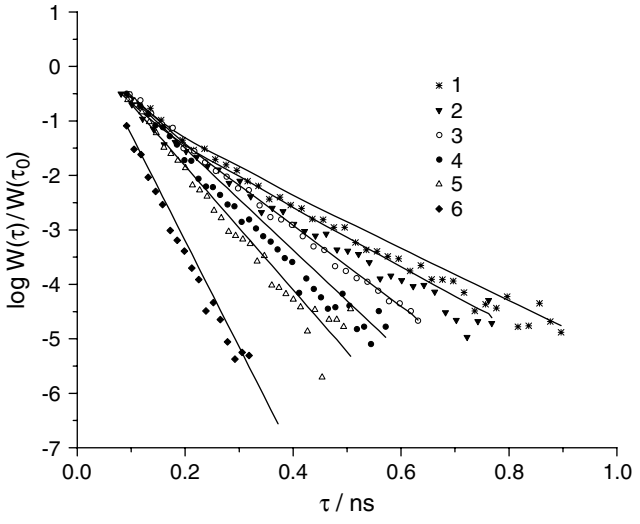

Figure 2. Raman coherence signals obtained on 1285 cm^{-1} band excitation ($T = 298$ K). Displayed are experimental (dots) and simulated (solid lines) values; gas densities: (1) 0.378; (2) 0.472; (3) 0.944; (4) 2.83; (5) 7.55; (6) 18.9 amagat.

OUTLINE OF THEORY

Since the CO_2 Q-branches have closely spaced fine structures and large rotational broadening cross-sections, the line mixing effects can be traced in a much wider range than for lighter linear rotators. A suitable characteristic is the 'reduced' band width[6] $\lambda = \langle \Delta\omega \rangle / \rho \langle \Gamma \rangle$, where $\langle \Gamma \rangle$ is the mean rotational broadening coefficient. The smallness of λ defines the approach to the motional narrowing limit where the rotational contribution to the bandwidth disappears linearly on λ.[6] Say, at a gas density $\rho = 10$ amagat, λ is ~0.1 for the 'red' component and 0.01 for the 'blue' component. For example, the isotropic Q-branch of nitrogen under this condition has $\lambda \approx 3$, which shows it to be very far from this limit. In contrast to diatomics, the vibrational relaxation distinctly manifests itself in the isotropic scattering spectra of compressed CO_2.

To a good approximation, one may assume the relaxation processes, except the vibrational ones, to be the same for both components. This allows us to apply the recently developed fast-collision approximation (FCA)[7] to both sets of measurements and therefore to arrive at a more consistent relaxation picture.

Signal simulation

The observed response $W(\tau)$ was calculated by a conventional procedure used in our previous study.[4] The Raman coherence $S(t)$ is excited by a two-color pump pulse with the envelope $I_{\text{pump}}(t)$:

$$S(t) = \int_0^\infty I_{\text{pump}}(t - t')G(t')\mathrm{d}t \tag{1}$$

where the Green function gives the response of the medium to a δ-pulse excitation. The probe pulse $I_{\text{probe}}(t)$ delayed by τ generates the signal whose power $W(\tau)$ is

$$W(\tau) = \int_{-\infty}^\infty I_{\text{probe}}(t)|S(t + \tau)|^2\mathrm{d}t \tag{2}$$

Green function

It is assumed that the relaxation channels of the molecular velocity (v), rotation (R) and vibration (V) are independent. Besides, there may exist losses (L) of coherently excited molecules which depart from the interaction volume before the probe pulse comes. The Green function then becomes

$$G(t) = C_{\text{v}}(t)C_{\text{R}}(t)C_{\text{V}}(t)C_{\text{L}}(t) \tag{3}$$

Velocity factor

This factor appears even in the ideal-gas case in which the velocity correlation time t_{V} is infinite. In this case, a Gaussian decay occurs with an effective time $t_{\text{D}} = (c/\omega_0)\sqrt{m/kT}$ (ω_0 is the vibrational transition frequency) because of the Doppler effect. In our case, $t_{\text{D}} \approx 4$ ns. The velocity correlation time

is related to the diffusion constant D: $t_V = Dm/kT\rho$. In the following, we apply the weak-collision model, for which

$$C_v(t) = \exp\{-a^2[1 - x + \exp(-x)]\} \quad (4)$$

where $x = t/t_V$ and $a = t_V/t_D$. It is the simplest model which gives an analytic expression based on measurable quantities.

Loss factor

The smallest time constant $t_D = r/\sqrt{kT/m}$ of this process is expected at the lowest densities for which the free-flight length l_0 exceeds the radius r of the interaction zone. Estimating r as 5×10^{-3} cm, one obtains a t_L value of the order of a few tens of nanoseconds. This makes the loss factor not very pronounced at the delays $t \leq 12$ ns used in our experiments. However, the question still remains open, because the loss factor in the collisionless regime can behave non-exponentially. It is expected that it should decrease faster at initial times because the molecules in the boundary zone can depart very quickly. The core particles fly from the area more slowly and $C_L(t)$ decays at large times by the power law. The losses are strongly damped at higher pressures ($\rho \geq \rho_0$), when $l_0 \leq r$ becomes valid. Estimations show ρ_0 to be $\sim 10^{-3}$ amagat in the CO_2 case. Therefore, the losses are negligible at densities used to study the 1285 cm^{-1} band and may slightly, if at all, affect the 1388 cm^{-1} signals recorded at two lowest pressures.

Vibrational factor

Since the delay time considerably exceeds the collision duration, one can write

$$C_V(t) = \exp[(-\gamma_V + i\delta_V)t\rho] \quad (5)$$

where γ_V and δ_V are, respectively, the vibrational broadening and shift coefficients. Under the conditions used, the shift does not affect the observed signals.

Rotational relaxation and fast-collision approximation

Generally, the rotational correlation function can be written as a scalar product in the line space

$$C_R(t) = \langle\langle I| \exp[(i\Omega - \Gamma)t]|I\rangle\rangle \quad (6)$$

The diagonal matrix Ω represents the set of fine-structure frequencies Ω_J and Γ is the rotational relaxation matrix. The vector $|I\rangle\rangle = \sum_J \sqrt{p_J}|JJ\rangle\rangle$ (representing the identity operator I) is defined via the line-space basis vectors $|JJ\rangle\rangle$ and the rotational populations p_J.

The FCA assumes the molecular orientation to remain unchanged during the collision duration and results in the following equation for the off-diagonal terms:

$$\Gamma_{JJ'} = -\exp(-\hbar\omega_{J'J}/2kT)\sqrt{(2J+1)(2J'+1)} \times \sum_{L>0} \begin{pmatrix} J & L & J' \\ 0 & 0 & 0 \end{pmatrix}^2 \Phi_L(\omega_{JJ'}) \quad (7)$$

where the conventional notation is used for the 3j symbols. In the general case (i.e. for a non-symmetric linear molecule), $L = 1, 2, 3, \ldots$, whereas for a centrosymmetric molecule (as in our case), $L = 2, 4, 6, \ldots$. In the latter case, the even-J and odd-J manifolds remain uncoupled by the relaxation.

The diagonal terms of Γ can be expressed in terms of the off-diagonal ones.[7] The positive real functions $\Phi_L(x)$ describe the evolution of the anisotropic terms during collisions. Their frequency dependence corrects for the finite rotational velocity and makes FCA superior to the conventional infinite-order sudden approximation (IOSA). In contrast to the commonly exploited energy-corrected sudden (ECS) approximation, the FCA matrix was derived non-empirically and was shown[7] to obey strictly the basic principles (sum rules, detailed balance, causality). In particular, the detailed balance demands that $\Phi_L(-x) = \exp(-\hbar x/kT)\Phi_L(x)$.

In the derivation of Eqn (7), it was tacitly assumed that the anisotropic interaction potential is not subject to the vibrational motion. This can be justified because the vibrational amplitudes are much smaller than the typical lengths characterizing the interaction. As the result, the collisional spectral functions Φ_L become independent of the vibrational quantum numbers specifying the band.

Equation (7) applies for the Q-branches observed in the isotropic Raman/CARS spectra of linear molecules making the $\Sigma \rightarrow \Sigma$ vibrational transition. In viewing of future FCA applications to other isotropic Raman/CARS bands, we generalize the results[7] on the case of the $\Pi \rightarrow \Pi$, $\Delta \rightarrow \Delta$, ... transitions. Correspondingly, the combining vibrational states have the same momentum projections $v = 1, 2, \ldots$ on to the symmetry axis. One then obtains

$$\Gamma_{JJ'} = -\exp(-\hbar\omega_{J'J}/2kT)\sqrt{(2J+1)(2J'+1)} \times \sum_{L>0} \begin{pmatrix} J & L & J' \\ v & 0 & -v \end{pmatrix}^2 \Phi_L(\omega_{JJ'}) \quad (8)$$

which means that line mixing at $v \neq 0$ requires the same input information as it does for the $\Sigma \rightarrow \Sigma$ bands. In the case considered, the bands are v-doubled, one sub-band having the odd J and the other having the even J. In contrast to Eqn (7), transitions with odd ΔJ are not forbidden and, therefore, both subbands are coupled by relaxation.

The complexity of the direct calculation of $\Phi_L(x)$ makes it necessary to model its form. We use in this study a model scheme which was successfully applied for nitrogen:[7]

$$\Phi_L(x) = A_L \frac{2}{1 + \exp(-\hbar x/kT)} \phi[x/\sqrt{1 + \chi L(L+1)}]$$

$$\phi(x) = \exp[\gamma - \sqrt{\gamma^2 + (xt_c)^2}]$$

As in the N_2 case, we assumed the basic ($0 \rightarrow L$) rates $Q_L = \Phi_L(\omega_{0L})$ to be given by the energy-gap law $Q_L = A\exp[-h(E_L/kT)]$, where h is a parameter. In so doing, the factor $Q_L/\Phi_L(\omega_{0L})$ enters the right-hand side of Eqn (8)

and the model is specified by five adjustable parameters $[A, \omega_c(\equiv t_c^{-1}), \gamma, \chi, h]$. In practice, simulated signals appear to be weakly sensitive to variations of γ and the latter was fixed ($\gamma = 1.5$) according to our previous findings;[7] as in the N_2 case, χ was also fixed: $\chi = 0.01$.

For nitrogen, the inverse collision duration found, $\omega_c \approx 100\ \text{cm}^{-1}$, prompts the relaxation rates to be defined by the repulsion forces. If this is also the case for CO_2, scaling of collision duration would give $\omega_c \approx 70\ \text{cm}^{-1}$. However, fittings of experimental CARS signals resulted in the ω_c values almost two times smaller. The interaction mechanism in the $CO_2 - CO_2$ case is, therefore, longer ranged than that relevant for pure nitrogen. This is consistent with a large value of the CO_2 quadrupole moment, which is three times larger than that of N_2. The quadrupole–quadrupole (QQ) contribution to Γ, while being small for pure nitrogen, is dramatically increased in our case. Since the QQ potential scales with the intermolecular separation as R^{-5}, whereas the repulsion term decreases approximately as R^{-12}, it is reasonable to assume that $\omega_c^{\text{rep}}/\omega_c^{\text{QQ}} \approx 2.5$. Correspondingly, the $\phi(x)$ function should be written as $\phi = \phi(x; t_c) + \alpha_Q \phi(x; 2.5t_c)$, where α_Q represents the relative role of the QQ term. Such a refined model incorporates α_Q as an adjustable parameter.

INTERPRETATION OF EXPERIMENTAL RESULTS

Some problems concerning the signal normalization appear, owing to (a) the finite pulse durations and (b) the nonresonant electronic term $G_{\text{el}}(t) \sim \delta(t)$, the amplitude of which is unknown. The convolutions with $I_{\text{pump}}(t)$ and $I_{\text{probe}}(t)$ [Eqns (1) and (2)] shift the maximum of $W(\tau)$ to a positive time value. For the electronic term dominating at very small time delays, a straightforward calculation shows the maximum of the response to be shifted by about $0.5\Delta_{1/2}$. This shift was incorporated in the experimental time-scale. Finally, to remove the electronic contribution, the normalization point τ_0 for both experimental and simulated responses was chosen to be 100 ps. This delay is large enough for the convolved electronic contribution to vanish, but too small for a considerable change of the slower response. Hence the quantity to be analyzed was defined by $Y(\tau) = \log[W(\tau)/W(\tau_0)]$.

The effects determining the transient shapes behave differently with respect to density and their roles are changed as the density is raised. As exemplified by the 1388 cm^{-1} band, the free-molecule response is superimposed at the lowest densities ($\rho \approx 10^{-3}$ amagat) by the Gaussian decay caused by the Doppler effect (Fig. 3). The latter is rapidly destroyed by increasing the collision frequency and becomes unimportant at $\rho \gtrsim 0.05$ amagat, as curve B in Fig. 3 shows. Below this density, both the velocity and rotational relaxation influence the observed signals. For both bands, the rotational relaxation is first accelerated by pressure; the acceleration

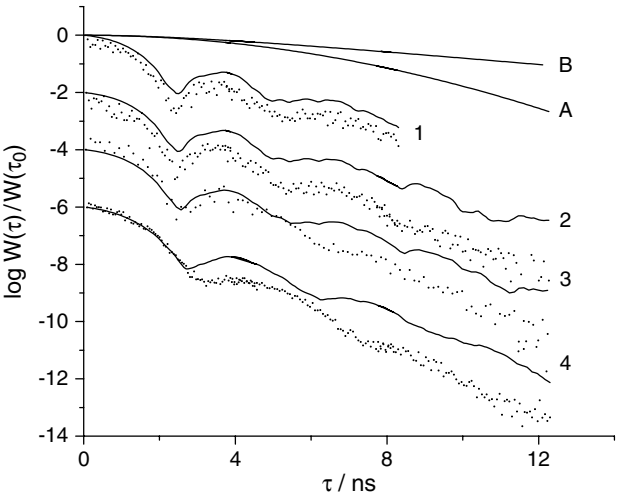

Figure 3. Raman coherence signals obtained on 1388 cm^{-1} band excitation ($T = 298$ K). Displayed are experimental (dots) and simulated (solid lines) values; gas densities: (1) 0.00062; (2) 0.0025; (3) 0.0076; (4) 0.0236 amagat. For clarity, curves 2–4 are sequentially shifted downwards by 2. Shown are velocity relaxation contributions at $\rho = 0$ (A) and 0.047 amagat (B).

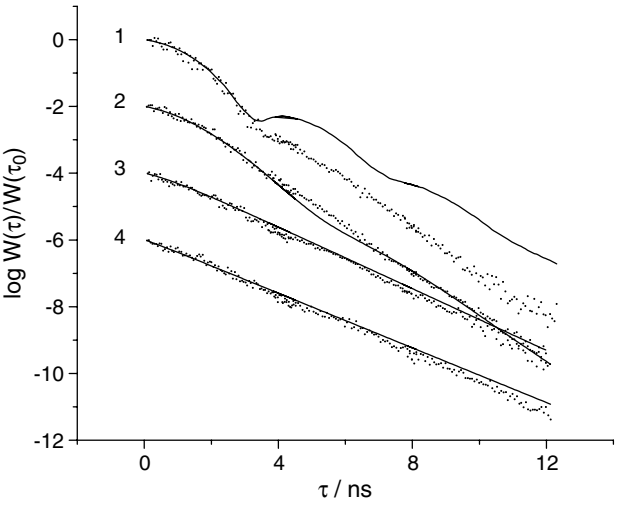

Figure 4. Similar plots as in Fig. 3. Densities: (1) 0.047; (2) 0.094; (3) 0.189; (4) 0.378 amagats.

reaches its maximum at $\lambda \approx 1$, after which the relaxation becomes progressively retarded. For the narrower 1388 cm^{-1} band this maximum rate is observed at rather low densities ($\rho = 0.05$–0.1 amagat, Fig. 4). For the broader 1285 cm^{-1} component, the maximum occurs at densities approximately 10 times larger, where it is partly masked by the vibrational relaxation (Fig. 2) monotonically increased by pressure. In the frequency domain, the acceleration and retardation stages correspond to line broadening and motional narrowing. At higher densities (~1 amagat), the vibrational effects become dominating for both bands (Figs 2 and 5).

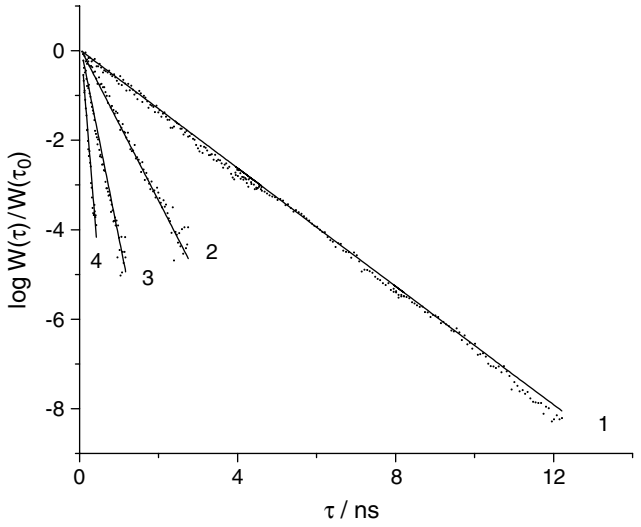

Figure 5. Similar data as in Fig. 3. Densities: (1) 0.944; (2) 2.83; (3) 7.55; (4) 18.9 amagats.

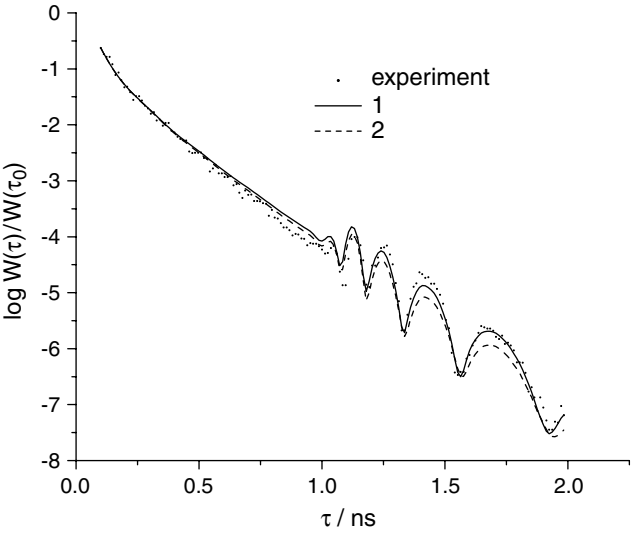

Figure 6. Simulations of the 1285 cm^{-1} coherence decay at $\rho = 0.047$ amagat. (1) Local fitting; (2) global fitting when all 1285 cm^{-1} data are processed.

A FORTRAN code was developed to simulate the CARS responses to account for all aforementioned effects. The probe and pump pulses were assumed to be Gaussian. The known diffusion constant $D = 0.15$ cm^2 amagat s^{-1} was used to model the velocity relaxation. The band spectroscopic constants were taken from Ref. 3. Diagonalization of the complex matrix $\Omega + i\Gamma$ was used to calculate the rotational Green function [Eqn (6)], which generally contained four varied parameters (A, ω_c, h, α_Q). The vibrational rate constants, different for both bands, were also included in fittings of the normalized functions $Y(\tau)$.

It was found that the 1388 cm^{-1} responses, when fitted separately, do not allow one to determine reliably the Γ-matrix parameters. This occurs because the band is easily narrowed and becomes mostly defined by a single quantity, the mean value of Γ^{-1}. The uniqueness of the derived rotational parameters is therefore lost. From this standpoint, the broader 'red' component is more promising and its responses were used further for analysis.

For any particular density, where the rotational contribution is important, the theory reproduces the 1285 cm^{-1} signals with high accuracy, as exemplified by Fig. 6 (curve 1). The agreement becomes poorer, though remaining reasonable, when all ''red'' band responses are fitted at once (Figs 1 and 2). The optimized FCA parameter values are following: $A = 7.73 \times 10^{-3}$ cm^{-1} $amagat^{-1}$, $\omega_c = 55$ cm^{-1}, $h = 0.957$, $\alpha_Q = 1.01$. The latter value shows the short- and long-range terms to contribute equally to the rotational rates.

The 1388 cm^{-1} signals were processed using the thus derived Γ-matrix and only γ_V was varied. Table 1 presents the vibrational rates for both bands and the values obtained by applying the frequency-domain CARS or related non-linear techniques at similar pressures. As can be seen, the results are scattered, with the time-domain technique resulting in higher rate constants.

Although the 1285 cm^{-1} data demonstrate overall good agreement between theory and experiment, the signal simulated at $\rho = 4.7 \times 10^{-2}$ amagat (curve 2 in Fig. 1) decays noticeably slower than the observed signal. We note that at higher densities the velocity relaxation vanishes rapidly and has no effect on the observed signals, as plots A and B in Fig. 3 demonstrate. At lower densities, the responses can be influenced by both the velocity and rotational relaxation. In this range, the 1388 cm^{-1} band responses are more informative because they were recorded at longer times. It is in this density interval where the largest regular deviations of the simulated and measured profiles are observed (curves 2–4 in Fig. 3 and curve 1 in Fig. 4). As in the case of the 1285 cm^{-1} band, the simulated signals decay more slowly than the observed signals, which cannot be compensated by variations of the velocity correlation time. As was estimated above, the loss factor does not play a noticeable role at these densities. Nor can it be due to the FCA drawbacks: this model reproduces the broadening coefficients (i.e. the

Table 1. Vibrational relaxation rate constants

Parameter	This study	Ref. 8	Ref. 9	Ref. 10
γ_V (1285 cm^{-1})/mK $amagat^{-1}$	5.7(1)	5.6(1)	4.1(4)	5.2(1)
γ_V (1388 cm^{-1})/mK $amagat^{-1}$	3.8(1)	3.1(1)	2.8(1)	—

diagonal part of Γ that defines the decay in the considered pressure range) with reasonable accuracy. In our opinion, the imbalance suggests that there exists a constructive interference between the relaxation channels disregarded in our approach. Physically, a collision is a common source of all considered relaxation channels and this makes them to some extent correlated. To our knowledge, the relevant theory is still lacking.

CONCLUSION

The studies of picosecond time-domain CARS responses recorded in a broad dynamic range offer a severe test of theoretical models of collision-induced relaxation processes. By scanning the gas density, such studies allow one to separate contributions from these processes and to reveal finer effects which are not so transparent for the frequency-domain techniques. Further investigations might result in a physical picture of correlated relaxation channels.

Acknowledgment

The authors thank the Russian Foundation for Basic Research (projects 01-02-16044 and 01-03-32744) for supporting this study.

REFERENCES

1. Kiefer W (ed.). *J. Raman Spectrosc.* 2000; **31**(1–2): (special issue devoted to femtosecond coherent Raman spectroscopy).
2. Akhmanov SA, Koroteev NI, Magnitskii SA, Morozov VB, Tarasevich AP, Tunkin VG. *J. Opt. Soc. Am. B* 1985; **2**: 640.
3. Rothman LS. *Appl. Opt.* 1986; **25**: 1795.
4. Kuznetsov DS, Morozov VB, Olenin AN, Tunkin VG. *Chem. Phys.* 2000; **257**: 117.
5. Andreev AV, Valeev AA, Morozov VB, Olenin AN, Tunkin VG. *Quantum Electron.* 2002; **32**: 54.
6. Burshtein AI, Temkin SI. *Spectroscopy of Molecular Rotation in Gases and Liquids*. Cambridge University Press: Cambridge, 1994; Chapt. 3.
7. Kouzov AP. *Phys. Rev. A* 1999; **60**: 2931.
8. Lavorel B, Millot G, Saint-Loup R, Berger H, Bonamy L, Bonamy J, Robert D. *J. Chem. Phys.* 1990; **93**: 2176, 2185.
9. Boulet C, Bouanich J-P, Hartmann J-M, Lavorel B, Deroussiaux A. *J. Chem. Phys.* 1999; **111**: 9315.
10. Kouzov AP, Kozlov DN, Hemmerling B. In *Book of Abstracts, European CARS Workshop, Heidelberg*, 1997; B-20.